Minor and trace element chemistry of carbonates, apatites and magnetites in some African carbonatites

J. B. Dawson

Department of Geology and Geophysics, University of Edinburgh, West Mains Road, Edinburgh EH9 3JW, UK

I. M. Steele, J. V. Smith

Department of Geophysical Sciences, University of Chicago, 5734 S. Ellis Ave, IL 60637, USA

AND

M. L. Rivers

Department of Geophysical Sciences and Consortium for Advanced Radiation Sources, University of Chicago, 5734 S. Ellis Ave, Chicago, IL 60637, USA

Abstract

In calcites and dolomites in seven African carbonatites, SrO, FeO and MnO occur in concentrations from 1 to 2 wt.%, whereas Ce, Y, Cu and Zn occur only at the ppm level. Sr, Ce and Y partition preferentially into calcite relative to co-existing dolomite, whereas Fe and Mn favour dolomite. Sr partitions preferentially into calcite relative to co-exisiting apatite, but the light rare-earth elements partition into apatite. Magnetite from Kerimasi contains up to 13 wt.% MgO and 6 wt.% MnO, extending the known ranges in composition of magnetites from carbonatites.

KEYWORDS: mineral chemistry, carbonatite, carbonate, apatite, magnetite, Africa.

Introduction

CARBONATITES are the crystalline products of low-volume, high-temperature carbonate melts that have evolved from the upper mantle for at least the past 2 Ga. Many are associated with crustal complexes of alkali-rich silicate rocks from which they may have evolved by liquid immiscibility (Le Bas, 1989), whereas others may have been directly generated in, and rapidly transported from, the upper mantle (Wallace and Green, 1988; Bailey, 1989, 1993). Despite the potential importance of carbonatites in providing information on the rare-metal budget of the upper mantle, most available chemical data are for bulk rocks and the relatively-minor but economically-important phases such as pyrochlore and monazite. Some bulk analyses are compromised because there is isotopic evidence of sub-solidus re-equilibration, often with meteoric water. By contrast, there is an overall paucity of information on the minor and trace elements in the more common phases in these rocks – the carbonates, apatite and magnetite-rich spinel, though some recent studies have addressed individual Brazilian, Indian and Chinese carbonatites (Morbidelli et al., 1986; Le Bas and Srivastava, 1989; Le Bas et al., 1992). Here we present electron-and X-ray microprobe data for the carbonates, apatites and magnetites in thirteen carbonatite samples from seven African complexes.

Specimen description

The carbonatite complexes range in age from Archaean to Quaternary, and descriptions of the individual complexes are given in the following publications; Phalaborwa (Archaean – 2 Ga, Eriksson, 1989), Goudini (Proterozoic? – Verwoerd, 1967), Tundulu Hill (Upper Jurassic – Garson, 1962), Panda Hill (Lower Cretaceous – Van Straaten, 1989), Tororo and Sukulu (Cretaceous – Davies, 1956), and

TABLE 1A. Summary of mineralogy

Sample	Cal	Dol	FeCO$_3$	Mag	Ap	BaSO$_4$	SrCO$_3$	FeS	Bio	Ksp	Ol/Humite
South Africa											
S387 Phalaborwa	x	x	-	x	-	-	-	-	-	-	-
S388 ditto	x	x	-	x	x	x	-	-	x	-	x
S240 Goudini	x	x	-	x	-	-	-	-	-	-	x
Malawi											
M26 Tundulu Hill	x			x	x	x	x	-	x	x	-
M28 ditto	x	-	-	x	x	-	x	-	x	-	-
Tanzania											
BD724 Panda Hill	x	x	-	-	x	-	x	-	-	-	-
BD892 Kerimasi	x	x	-	x	x	-	-	-	-	-	x
BD893 ditto	x	-	-	x	x	-	-	-	x	-	-
Uganda											
U47 Tororo	x	-	-	x	x	-	-	x	-	-	-
U48 ditto	x	-	x	x	x	x	-	x	-	x	-
U51 ditto	x	-	x	x	x	x	x	x	-	-	-
U58 ditto	x	-	-	-	x	-	-	x	-	-	-
U63 Sukulu	x	x	-	-	x	-	-	-	x	-	-

Kerimasi (Quaternary – Dawson, 1964). Most are well-eroded plutonic complexes, but Kerimasi is a young (<1.2 Ma) pyroclastic volcano from which the studied specimens are ejected blocks. The two specimens from Kerimasi have whole-rock Sr and Nd isotope values similar to ocean-island basalts (Paslick *et al.*, 1995). Apart from the exotic blocks at Kerimasi, the samples are from the major carbonatite units within the complexes. All were selected from a suite investigated by Sheppard and Dawson (1973); the δ^{13}C and δ^{18}O isotope values of −4 to −9‰ and 6 to 8.5‰ respectively, indicate they have not interacted with high-level crustal or meteoric fluids.

The mineralogy, determined by a combination of light-optics examination, qualitative EDS analysis and back-scattered electron imaging, is summarised in Tables 1A, 1B. The carbonatites fall into two main groups – those containing appreciable quantities of dolomite, and others that are dolomite-free. Minor strontianite occurs in some members of both groups, and accessory FeCO$_3$ occurs in two specimens from Uganda.

Several specimens show signs of deformation, manifest by uneven grain size and bent twin- or glide-planes, or contain strongly oriented inequidimensional carbonate and apatite grains; only the specimens from Tundulu Hill, Panda Hill and Kerimasi contain strain-free carbonate grains of equal size.

The specimens from Phalaborwa and Panda Hill contain exsolved carbonate. In the Panda Hill sample are two calcites — clear high-Sr calcite, and cloudy, low-Sr calcite the cloudiness of which results from numerous tiny grains of exsolved strontianite (Fig. 1a). In the Phalaborwa rocks, the dominant calcite contains exsolved rods and blebs of dolomite (Fig.1b) similar to examples reported by Goldsmith (1960) and Van der Veen (1965). The calcite also contains minute grains of another exsolved phase that was detected during BSE imaging (Fig. 1c); these grains are generally <5 μm, equidimensional, and intermediate between calcite and dolomite in composition (Ca$_{61}$Mg$_{39}$). Further, the central parts of some of the exsolved dolomite grains contain clouds of minute high-Sr calcite grains (Fig. 1d). Hence, for the Phalaborwa carbonatites, we infer two stages of exsolution, the first giving rise to the gross calcite–dolomite perthite, and the second resulting in the partial expulsion of small amounts of residual Mg and Ca+Sr from the lattices of the two main exsolved phases.

Mineral chemistry

The minerals were analysed on a Cameca SX50 electron microprobe at the University of Chicago, using wavelength dispersive spectrometers with matrix correction by PAP procedure. For the

TABLE 1B. Mineralogical comments

S387. Calcite contains two exsolved carbonates: (a) rod-shaped, sigmoidal or rounded dolomite grains (perthitic texture); and (b) a phase compositionally intermediate between calcite and dolomite (referred to as magnesio-calcite) forming abundant, angular, equidimensional grains, generally not greater than 2−3 mm, that has a higher BSE intensity. Central parts of some dolomite grains contain 10 × 1 μm elongate grains of Sr-calcite ± SrSO$_4$ ± *REE* phosphate. Tiny grains of Ce,La carbonate in calcite. In both *REE* phases Ce > La > Nd. Also Fe,Cu,S phase.

S388. Carbonates as in S387. Calcite-dolomite exsolution textures are even more pronounced, with grains of magnesio-calcite less abundant but up to 20 μm. Also large (up to 10 mm) grains of humite; mica up to 100 μm included in humite; monazite; Pb-bearing thorianite; Ca*REE* silicate; baddeleyite.

M26. Two calcites; clean cc has Sr,Mn,Fe; cloudy cc is cc+ exsolved Sr-cc + sub-micron blebs of a phase enriched in Fe and Mn (? carbonate) ± SrCa phase. Also Ca-SrSO$_4$.

M28. Two calcites, Sr-cc and cc+exsolved strontianite. Also minor discrete Sr-CaCO$_3$ and SrSO$_4$.

BD724. Two calcites, Sr-cc and cc+strontianite. Dolomite grains small and cuspate. Complex intergrowths of Ce*REE* carbonate, Ca*REE* Pb carbonate, celestite and baryte; Sr baryte.

BD892. Small, cloudy dolomite grains; Ba,Fe,Ca,S,Si,Mg phase; Mn-bearing forsterite contains 15−20 μm rounded or amoeboid areas of humite; magnetite contains high Mg and Mn, low Ti, Al, V. Dolomite, magnetite and apatite are concentrated in oriented, discontinuous micro-fractures.

BD893. Mica is Ti-phlogopite. Magnetite contains Mn.

U47. Ca-Fe amphibole replaced by fine intergrowths of FeCO$_3$ + FeS$_2$ + cc + qtz.

U48. Apatite-FeS-FeCO$_3$+CaCO$_3$ intergrowths; large Ksp.

U51. Pseudomorphs as in U47.

U58. Ca Fe amphibole; Nb-TiO$_2$; FeS$_2$?; Si,Ca,Ti phase.

U63. Dolomite grains small and cuspate. One Nb-Ta-U grain; Ce,CaCO$_3$.

---

carbonates, electron beam conditions were chosen to minimize loss of Ca and Mg during analysis. In test runs, there was a 5% increase in the counts for Ca in calcite over a 5-minute period (20 μm diameter beam, 50 nA incident current and 15 kV accelerating potential); there was no change in the counts for Ca and Mg in dolomite. Other phases were analysed with a 10 μm beam. Additional X-ray microprobe analyses for trace elements in selected specimens were made at beamline X26A of the National Science Laboratory Synchrotron Facility at Brookhaven, New York. The synchrotron XRF technique is described by Smith (1995)

Carbonates. All the calcites and dolomites contain significant concentrations of FeO, MnO and SrO (Table 2). Concentrations of FeO and MnO are quite constant (Fig. 2), with the exceptions of (*a*) dolomite in the Panda Hill carbonatite (724) that shows a range in MnO concentrations, and (*b*) calcite from Tundulu Hill (M26); in both specimens there are variations in both FeO and MnO, with the relatively low Mn and Fe being in grains that have exsolved strontianite (Fig. 3). The SrO in calcite grains within a given specimen can be variable depending upon whether there has been exsolution of minute grains of strontianite (Fig. 4). Overall, the calcites contain less FeO and MnO than co-existing dolomites and, when exsolution of strontianite has not occurred, they contain more SrO. Ferroan dolomite (FeO 3.04 wt.%) containing 0.10 wt.% Zn occurs in one of the Ugandan carbonatites.

With the exception of Kerimasi carbonatite BD 892, partitioning of FeO, MnO and SrO between calcite and co-existing dolomite appears to be
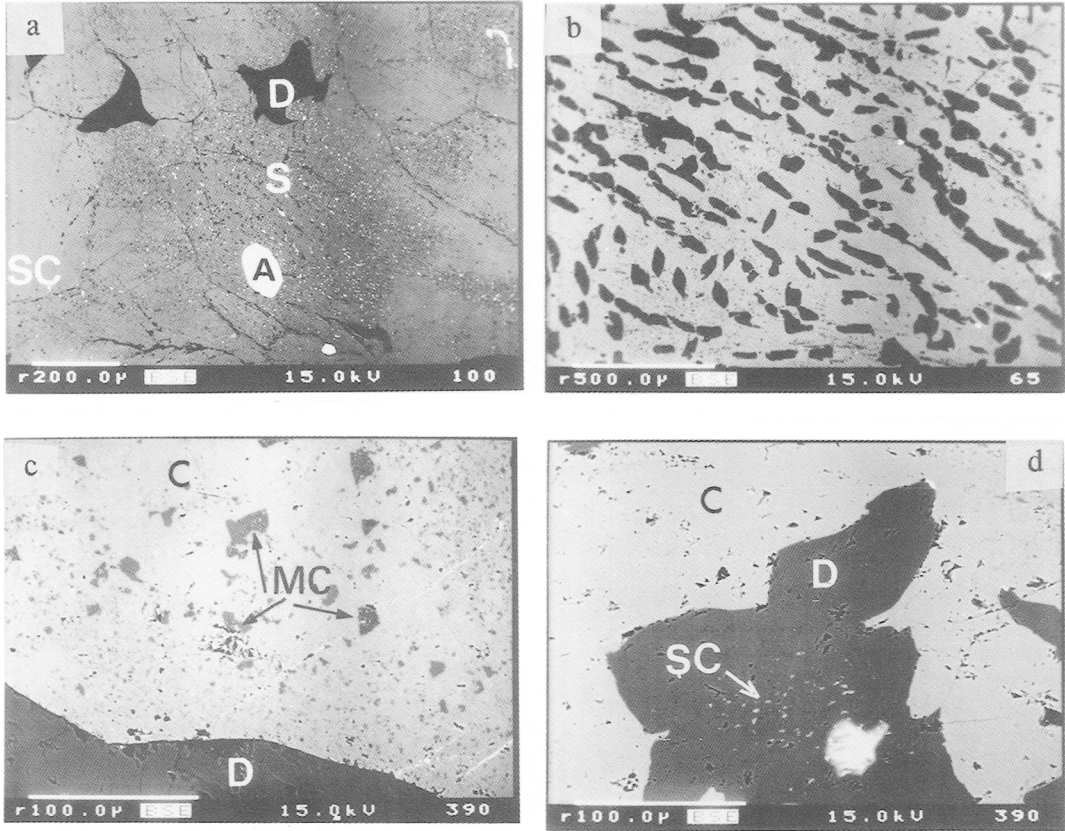
FIG. 1(a) BSE image of BD724 from Panda Hill. Clear high-Sr calcite (SC: 1.26 wt.% SrO)) contrasts with cloudy low-Sr calcite (S: 0.41 wt.% SrO) that contains numerous minutes grains of white stontianite. Dolomite (D) and apatite (A) are also present. (b) BSE image showing oriented lamelle of exsolved dolomite (black) in calcite (light grey) in carbonatite S388 from Phalaborwa. The calcite contains clouds of minute dark-grey inclusions of high-Mg calcite ($Ca_{61}Mg_{39}$); see Fig.1c. (c) Enlargement of part of Fig. 1b. Exsolved grains of high-Mg calcite (MC - $Ca_{61}Mg_{39}$) are set in calcite C ($Ca_{95}Mg_5$). D is dolomite. (d) Enlargement of a different field-of-view in S388. Cloud of exsolved high-Sr calcite (SC) in area of exsolved dolomite (D). The SC contains 1.28 wt.% SrO compared with 1.00 wt.% in the main calcite (C).

reasonably constant (Table 3) with K_DFeO 0.09 − 0.12, K_DMnO 0.54 − 0.64, and K_DSrO 2.3 − 2.6 (K_D being wt.% oxide in calcite divided by the wt.% oxide in co-existing dolomite). This constancy of partitioning is independent of the absolute concentrations. The atypical Fe and Mn partitioning in BD892, and the particularly low Mn and Fe concentrations in both carbonates, is possibly complicated by the presence of magnetite that is exceptionally high in MgO and MnO (12.9 and 6.06 wt.% respectively). Further, the unusually low K_DSrO (1.1) in this specimen is due to unusually-high SrO in the dolomite.

TABLE 3. Minor element partitioning between carbonatite carbonates

Specimen	K_DFeO	K_DMnO	K_DSrO
S387	0.08	0.55	2.3
S388	0.09	0.64	2.3
S240	0.12	0.54	2.6
BD724	0.11	0.61	0.78*−2.4
BD892	0.03	0.25	1.1
U63	0.12	0.54	2.6

* calcite in association with $SrCO_3$

K_D = wt.% oxide in calcite/wt.% oxide in dolomite.

TABLE 2. Representative analyses of calcite (C) and dolomite (D) from carbonatites

	S387-C[‡]	S387-C[‡‡]	S387-D	S388-C	S388-SC[†]	S388-D	S388-MC[††]
MgO	2.00	0.35	20.2	1.94	4.10[¶]	20.0	16.1
CaO	53.2	55.2	29.9	52.3	56.3	30.2	35.3
MnO	0.06	0.08	0.09	0.09	0.11	0.14	0.30
FeO	0.17	0.05	1.21	0.13	0.40	1.42	1.22
SrO	0.92	0.65	0.43	1.00	1.28	0.42	0.70
Total	56.35	56.33	51.83	55.46	62.19	52.18	53.62
Ca:Mg	95:5	99:1	52:48	95:5		52:48	61:39

	S240-C	S240-D	M26-C*	M26-C**	M26-C**	M28-C*	M28-C**
MgO	1.20	21.2	0.36	0.06	0.09	0.19	0.19
CaO	53.4	30.2	50.6	52.6	54.3	50.9	51.1
MnO	0.07	0.13	1.69	1.24	0.23	0.70	0.70
FeO	0.04	0.33	1.73	0.58	0.56	0.70	0.76
SrO	0.47	0.18	1.74	0.17	0.38	2.68	1.78
Total	55.18	52.04	56.12	54.65	55.56	55.17	54.53
Ca:Mg	97:3	51:49	99:1	100:0	100:0	99:1	99:1

	BD724-C*	BD724-C**	BD724-D	BD892-C	BD892-D	BD893-C	U47-C
MgO	0.88	0.23	19.0	0.17	22.3	0.07	0.05
CaO	51.3	52.6	29.1	54.6	29.0	54.6	53.8
MnO	0.71	0.63	1.16	0.03	0.12	0.03	0.15
FeO	0.29	0.14	2.51	0.01	0.26	0.02	0.19
SrO	1.26	0.41	0.48	0.70	0.60	0.57	0.81
Total	54.44	54.01	52.25	55.51	52.42***	55.29	55.00
Ca:Mg	98:2	99:1	52:48	100:0	48:52	100:0	100:0

	U48-C	U51-C	U58-C	U63-C	U63-FD
MgO	0.04	0.07	0.11	0.68	19.2
CaO	53.6	53.1	54.2	52.8	29.7
MnO	0.17	0.30	0.28	0.20	0.36
FeO	0.14	0.42	0.28	0.37	3.04
SrO	0.79	0.55	0.59	0.63	0.25
Total	54.74	54.44	55.46	54.68	52.65****
Ca:Mg	100:0	100:0	100:0	98:2	53:47

[‡] S387 main calcite. [‡‡] S387 tiny grains of calcite exsolved from dolomite; MgO ranges 0.19 to 0.62 wt.%, SrO ranges 0.65 to 0.98 wt.%; minute grains of $SrCO_3$ at interface with dolomite.
[†] S388-SC is 3 μm grain of high-Sr calcite exsolved from dolomite; [¶] high Mg is erroneous, resulting from beam overlap with surrounding dolomite.
[††] S388-MC is magnesio-calcite exsolved from calcite.
* 'Primary' calcite. ** Calcite containing 'clouds' of fine-grained, exsolved $SrCO_3$.
*** Total includes 0.14 wt.% ZnO. ****U63-FD is ferroan dolomite; total contains 0.10 wt.% ZnO.

Minor amounts of Ba, Al and Si (up to 0.40, 0.58 and 0.85 wt.% respectively) were reported in carbonatite calcites and dolomites by Quon and Heinrich (1966). Their samples were analysed by
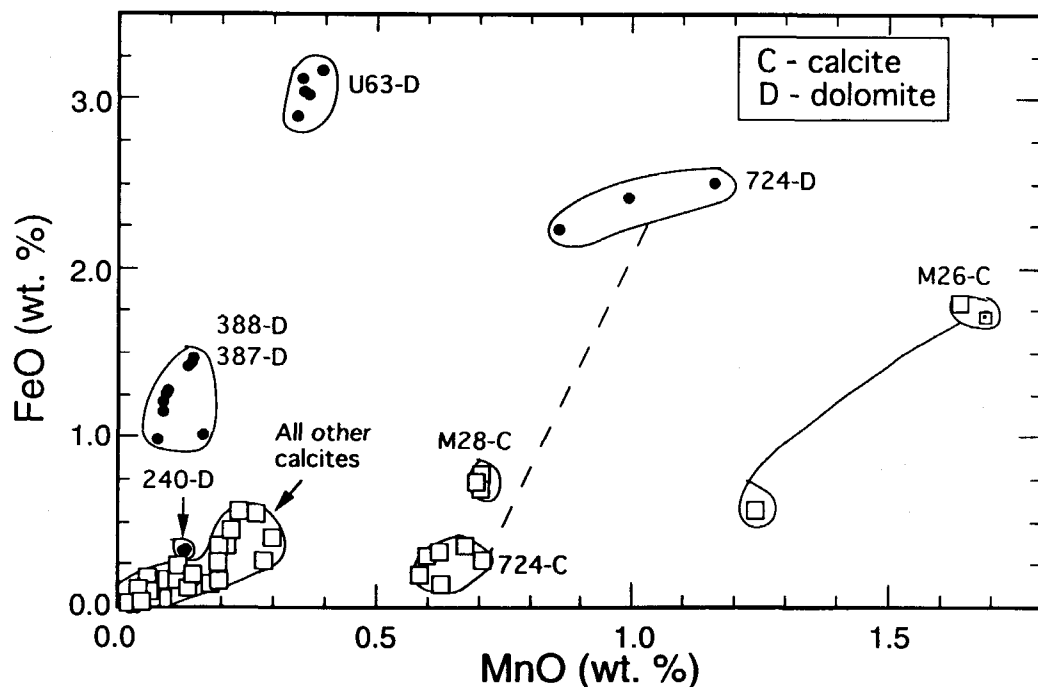
FIG. 2. Plot of FeO *vs.* MnO in calcites (square ornament) and dolomites (filled circles).

optical spectrography after hand-picking carbonate grains from crushed rocks. We specifically analysed for these elements (by electron probe), but they were below the level of detection in all our samples.

Individual phases in polished sections of five samples were analysed by XRF microprobe techniques. Because accuracy is critically dependent on sample thickness,especially for elements with X-ray energies about 6 keV, even small variations in thickness preclude quantitative results. However, if the sections are assumed to be of the same thickness, intensities can be compared on a relative basis to derive partition relations and variation among phases in different carbonatite samples. A typical XRF spectrum for dolomite in BD892 is shown in Fig. 5. Correlation of data for Mn and Fe obtained by the electron and XRF microprobes agreed within a factor of two and, considering exsolution and possible zoning, this variation is not unexpected. A similar variation for Ce, Cu and Zn is assumed. Absolute values for Y (because of its high energy) will be greater. Results are given in Table 4. Ce concentrations are up to 250 ppm, Cu 5 ppm, Zn 12 ppm and Y 142 ppm in calcites, and up to 107, 4, 10 and 110 ppm respectively in the co-existing dolomites. Ce and Y partition preferentially into calcite whereas Cu and Zn shown no obvious preference but their low

TABLE 4. Trace elements in carbonatite phases (analysis by X-ray microprobe)

	Ce	Cu	Zn	Y
S388 calcite	250	3	3	140
S388 *dolomite*	90	1	4	100
S388 apatite	1700	6	2	230
S240 calcite	110	2	2	70
ditto	105	7	2	55
S240 dolomite	25	3	3	30
ditto	40	3	3	30
BD892 calcite	140	4	10	50
ditto	60	5	3	50
U63 calcite	170	3	5	100
U63 dolomite	105	1	6	45
ditto	110	4	10	110
U63 apatite	5700	15	10	90
U58 calcite	180	3	3	40

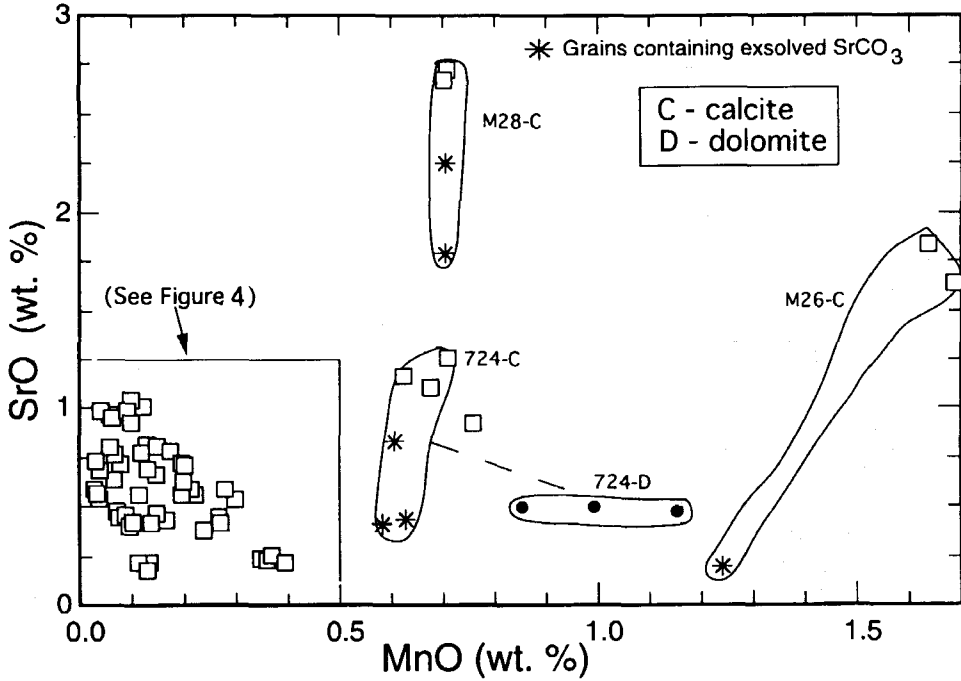Detection limits: Ce and Y - 1.0 ppm, Cu and Zn - 0.5 ppm.

FIG. 3. Plot of SrO *vs.* MnO. Symbols in main part of diagram as in Fig. 2. (Symbols in low-SrO, low MnO area are non-specific).
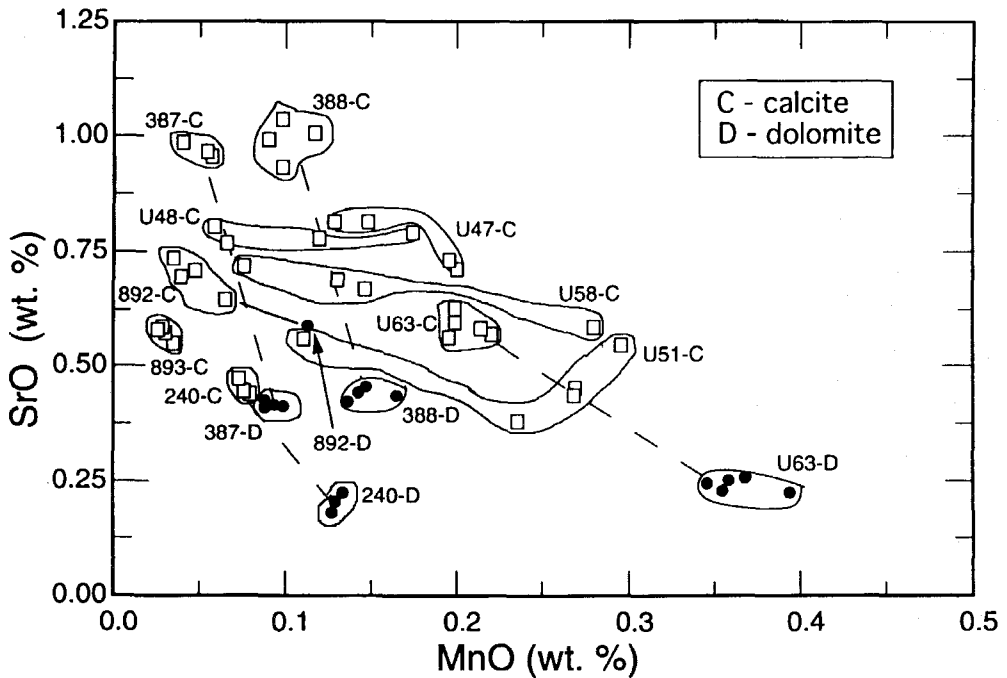

FIG. 4. Enlargement of low-Sr, low-Mn area of Fig. 3. Dashed lines connect co-existing calcite-dolomite.

TABLE 5. Representative apatite analyses from carbonatites

	S388	M26	M28	BD724	BD892	BD893
P_2O_5	42.2	41.9	42.1	42.8	42.1	41.5
CaO	54.5	53.1	51.6	53.8	54.6	55.4
SrO	0.73	2.450	2.25	0.65	0.41	0.35
MnO	0.01	0.06	0.06	0.06	0.01	0.01
FeO	0.0	0.06	0.05	0.03	0.01	0.0
Ce_2O_3	0.34	0.54	0.85	0.23	0.20	0.18
La_2O_3	0.15	0.23	0.39	0.11	0.10	0.16
Nd_2O_3	0.25	0.23	0.36	0.11	0.06	0.02
Na_2O	0.10	0.22	—	—	0.07	—
Cl	0.14	0.01	0.0	0.01	0.01	0.01
F	2.39	2.89	2.12	1.69	2.17	1.90
$O \equiv F$	1.01	1.22	0.89	0.67	0.91	0.80
Total	99.80	100.47	98.89	98.82	98.83	98.73

	U47	U48	U51	U58	U63
P_2O_5	42.7	42.8	42.2	41.9	42.5
CaO	54.8	54.6	54.9	55.0	54.8
SrO	0.49	0.62	0.64	0.42	0.39
MnO	0.03	0.01	0.02	0.02	0.04
FeO	0.01	0.01	0.01	0.02	0.03
Ce_2O_3	0.13	0.14	0.12	0.26	0.11
La_2O_3	0.08	0.08	0.07	0.13	0.05
Nd_2O_3	0.06	0.04	0.04	0.10	0.08
Na_2O	0.13	—	0.19	—	0.11
Cl	0.0	0.0	0.0	0.01	0.01
F	2.32	2.23	2.16	1.98	1.87
$O \equiv F$	0.98	0.94	0.91	0.83	0.79
Total	99.77	99.59	99.44	99.01	99.20

values limit interpretation beyond being present in detectable concentrations.

Apatite. As in most earlier reports of the chemistry of carbonatite apatites (reviewed by Hogarth, 1989), the apatites are fluor-apatites (F is generally ~ 2 wt.%), containing only small amounts of Na_2O (Table 5). The main minor oxide is SrO (0.41 – 2.45 wt.%) with the highest concentrations being in the Tundulu apatites (up to 2.45 wt.%). All apatites contain relatively high Sr combined with low Mn which is characteristic of carbonatite apatites compared with those in granite pegmatites, phosphorites and skarns (Hogarth, 1989). In several apatites the heavy *REE* were at, or below, detection limits, so only the light *REE* Ce, La, and Nd were analysed. Ce is in the highest concentrations, followed by La and Nd. As with Sr, the highest concentrations are in the Tundulu apatites with up to 0.85, 0.39 and 0.36 wt.% of the Ce, La and Nd oxides respectively.

With the exception of apatite in one Tundulu specimen (M26), apatite always contains less SrO than coexisting primary calcite (i.e. not containing exsolved strontianite). Conversely, where the light *REE* Ce, La and Nd are in sufficient concentrations in the apatites to permit electron microprobe analysis, only Ce could be detected at the ppm level by X-ray microprobe analysis (Table 4). Thus calcite is the main site of Sr in the studied carbonatites, and apatite the main site for the *REE*.

Magnetite. The magnetites (Table 6) are mainly magnetite-magnesioferrites containing only very small concentrations of Zr, V and Nb. They show considerable variation in their Ti, Al, Mn and Mg concentrations, both between specimens from individual localities and between localities. Those from the Tundulu specimens are relatively pure, with only trivial amounts of these minor elements; those from Phalaborwa contain small amounts, but high concentrations are found in the Kerimasi magnetites, one
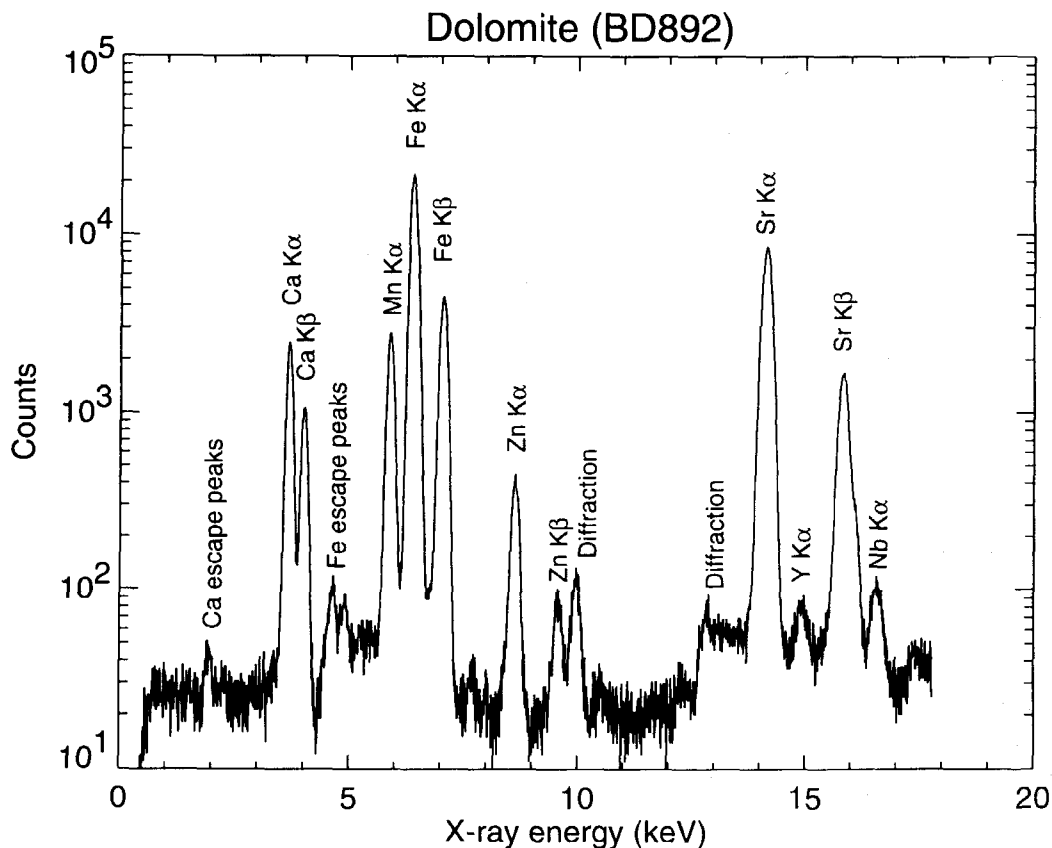
FIG. 5. Typical energy dispersive spectrum of dolomite in BD892 from XRF microprobe. Peaks with energies less than about 3 keV are highly absorbed and do not appear in the spectrum. Diffraction peaks are due to chance orientation of detector and diffracting plane in sample to record a specific energy from the continuum incident X-ray beam.

of which (from BD892) contains 12.9 wt.% MgO, 6.06 MnO, 5.14 Al_2O_3 and 1.55 % TiO_2; individual grains within this specimen show significant variations in Ti, Al, and total Fe, as well as in the ratio of FeO to (calculated) Fe_2O_3. The magnetite from the other Kerimasi specimen (BD893) also contains appreciable amounts of these oxides, but not in such high concentrations as in BD892. These Kerimasi magnetites are the most magnesian and manganoan yet recorded from carbonatite. Unfortunately, the exotic nature of these specimens (ejected blocks in pyroclastics) has precluded any interpretation as to their relationships, unlike the study by Gaspar and Wyllie (1983a) who found systematic variations in the compositions of magnetite-magnesioferrites in successive carbonatite intrusions in the Jacupiranga complex, Brazil.

The greatest variation within single grains is seen in the magnetites from the Goudini carbonatite in which large (500 μm) grains with cores containing relatively-high Al, Mn and Mg zone towards more iron-rich rims (Table 6, analyses 5,6); the cores of very small (40 μm) grains are even more iron-rich and contain higher concentrations of Mn than the rims of the larger grains. Prins (1972) records Fe enrichment in the rims of magnetites from several other African carbonatites, but this is accompanied by Mn depletion, the reverse of that found in the Goudini magnetites.

Ilmenite. The chemistry of carbonatite ilmenites has been reviewed by Mitchell (1978) and Gaspar and Wyllie (1983b) who identify two main groups, one group consisting of high-Mg ilmenites, mainly from the Jacupiranga and Oka carbonatites. In our

TABLE 6. Carbonatite magnetites

	1	2	3	4	5	6	7	8	9	10	11
TiO_2	0.52	0.00	0.12	0.22	0.23	0.19	0.14	2.18	1.55	2.26	0.54
ZrO_2	0.00	0.00	0.05	0.02	0.01	0.01	0.02	0.01	0.07	0.02	0.21
Cr_2O_3	0.02	0.02	0.03	0.01	0.03	0.00	0.01	0.02	0.01	0.00	0.03
Al_2O_3	0.16	0.24	0.02	0.02	1.55	1.17	0.61	1.31	5.14	6.58	3.13
V_2O_3	0.14	0.01	0.35	0.21	0.03	0.05	0.06	0.20	0.08	0.02	0.07
Fe_2O_3	69.60	69.51	67.99	68.58	69.76	69.10	68.68	64.81	67.14	63.77	71.59
FeO	28.78	30.85	30.82	31.19	21.03	26.42	27.50	24.08	7.48	6.62	7.48
MnO	0.16	0.02	0.00	0.05	0.55	0.32	1.81	3.76	6.06	5.92	6.08
MgO	1.92	0.32	0.00	0.01	6.34	3.09	1.26	3.43	12.90	13.00	12.20
Nb_2O_5	0.00	0.02	0.01	0.01	0.01	0.01	0.00	0.00	0.04	0.02	0.05
Sum	101.30	100.99	99.39	100.32	99.54	100.36	100.09	99.80	100.47	99.11	101.38

1. S388
2. S387
3. M28
4. M26
5. and 6. S240 - Centre and edge of 500 μm grain; 7. S240- centre of 40 μm grain
8. BD893
9. BD892 Representative analysis; 10 and 11 extremes of compositions.

specimens, ilmenite has only been found in specimen M28; its composition (Nb_2O_5 0.84, SiO_2 0.05, TiO_2 49.8, FeO 47.5, MnO 1.73, MgO 0.05, sum 99.96) falls within the low-Mg group of carbonatite ilmenites.

Silicates. Small quantities of olivine and humite have been found in three of the investigated carbonatites (Table 1). Detailed discussion of the compositions (Table 7) is beyond the scope of this paper, but the high concentrations of MnO in both the olivine and humite in BD892 are worthy of note in the context of the anomalous Mn partitioning between the carbonates in this particular sample; further, their high MgO concentrations mirror the high MgO in the Kerimasi magnetites.

Conclusions

1. SrO, FeO and MnO occur at minor element concentrations (0.1 to 2 wt.%) in many carbonatite calcites and dolomites, whereas Ce, Y, Cu and Zn occur at the ppm level.

2. Sr, Ce and Y partition preferentially into calcite relative to co-existing dolomite, whereas Fe and Mn favour dolomite. Cu and Zn show no strong preference.

3. Partitioning is never absolute, as calcite always contains small concentrations of Fe and Mn, and dolomite always contains small amounts of Sr and excess Ca, i.e. exsolution is never complete. In one Palaborwa specimen we have identified an exsolved CaMg carbonate of hitherto unknown composition Ca:Mg 61:39

4. With the exception of one carbonatite, partition coefficients (K_D = wt.% oxide in calcite/wt.% oxide in dolomite) are reasonably constant — K_D SrO = 2.3–2.6, K_D FeO = 0.08–0.12, and K_D MnO 0.54–0.64, despite the specimens being from carbonatites of different ages and the carbonates having variable absolute concentrations of these minor elements.

5. Ba, Al and Si have previously been reported in minor- or trace-element concentrations in analyses of bulk carbonates from carbonatites (Quon and

TABLE 7. Analyses of olivine and humite

	1	2	3	4
SiO_2	42.4	36.2	42.3	34.9
FeO	3.19	6.55	0.80	2.44
MnO	0.31	0.18	1.53	0.82
MgO	54.7	54.0	55.1	57.6
F	0.00	3.14	0.00	5.47
Less O $\equiv$ F	0.00	1.43	0.00	2.30
Sum	100.60	99.64	99.73	98.93

1. Forsterite, S240 Goudini.
2. Humite, S388, Phalaborwa.
3. and 4. Forsterite and humite, BD892 Kerimasi.

Heinrich, 1966). These elements were specifically sought, but not found in the present study by *in situ* analysis of individual carbonate grains. It is possible that the earlier reported concentrations may result from unidentified contaminants in the bulk samples.

6. SrO is preferentially concentrated in calcite, relative to coexisting apatite, whereas the light rare-earth elements partition preferentially into the apatite.

7. The high concentrations of MgO (13.0 wt.%) and MnO (6.06 wt.%) in the Kerimasi magnetites extend the known ranges in composition of carbonatite magnetites.

Acknowledgements

References

Bailey, D.K. (1989) Carbonate melt from the upper mantle in the volcanoes of south-east Zambia. *Nature*, **388**, 415–8.

Bailey, D.K. (1993) Carbonate magmas. *J.Geol. Soc. London,* 150, 637–51.

Davies, K.A. (1956) *The geology of part of south-east Uganda.* Geol. Surv. Uganda Memoir 8, 76pp.

Dawson, J.B. (1964) Carbonatitic volcanic ashes in northern Tanganyika. *Bull. Volcanol.*, 27, 81–92

Eriksson, S.C. (1989) Phalaborwa: a saga of magmatism, metasomatism and miscibility.In *Carbonatites* (K. Bell, ed.), Unwin Hyman, London, 105–48.

Garson, M.S. (1962) *The Tundulu carbonatite ring-complex in southern Nyasaland.* Geol. Surv. Nyasaland, Memoir **2**, 248 pp.

Gaspar, J.C. and Wyllie, P.J. (1983*a*) Magnetites in the carbonatite from the Jacupiranga Complex, Brazil. *Amer. Mineral.*, **68**, 195–213.

Gaspar, J.C. and Wyllie, P.J. (1983*b*) Ilmenite (high Mg, Mn, Nb) in the carbonatites from the Jacupiranga complex, Brazil. *Amer. Mineral.*, **68,** 960–71.

Goldsmith,J.R. (1960) Exsolution of dolomite from calcite. *J. Geol.*, **68**, 103–9.

Hogarth, D.D. (1989) Pyrochlore, apatite and amphibole: distinctive minerals in carbonatite. In *Carbonatites* (K. Bell, ed.), Unwin Hyman, London, 105–48.

Le Bas, M.J. (1989). Diversification of carbonatites. In: *Carbonatites* (K. Bell, ed.) Unwin Hyman, London, 427–47.

Le Bas, M.J. and Srivastava, R.K. (1989) The mineralogy and geochemistry of the Mundwara carbonatite dykes, Sirohi district, Rajasthan, India. *Neues Jahrb. Mineral. Abh.*, **160**, 207–27.

Le Bas, M.J., Keller, J., Tao Kejie, Wall, F., Williams, C.T. and Zhang Peishan (1992) Carbonatite dykes at Bayan Obo, Inner Mongolia, China. *Mineral. Petrol.,* **46**, 198–228.

Mitchell, R.H. (1978) Manganoan magnesian ilmenite and titanian clinohumite from the Jacupiranga carbonatite, Sao Paulo, Brazil. *Amer. Mineral.*, **63**, 544–7.

Morbidelli, L., Beccaluva, L., Brotzu, P., Conte, A., Garbarino, C., Gomes, C.B., Macciiotta, G., Ruberti, E., Scheibe, L.F. and Traversa, G. (1986) Petrological and geochemical studies of alkaline rocks from continental Brazil, 3 Fentization of jacupirangite by carbonatite magmas in the Jacupiranga Complex, SP. *Periodico di Mineralogia*, **55**, 261–95.

Paslick, C., Halliday, A., James, D. and Dawson, J.B. (1995) Enrichment of the continental lithosphere by OIB melts: isotopic evidence from the volcanic province of northern Tanzania. *Earth Planet. Sci. Letts.,* **130**, 109–26.

Prins,P. (1972) Composition of magnetites from carbonatites. *Lithos*, **5,** 227–40.

Quon Shi, H. and Heinrich, E.W. (1966) Abundance and significance of some minor elements in carbonatitic calcites and dolomites. *Mineral. Soc. India, Internat. Mineral. Ass. Volume*, (Papers 4th Gen. Meeting), 29–36.

Sheppard, S.M.F. and Dawson, J.B. (1973) $^{13}C/^{12}C$ and D/H isotope variations in "primary" igneous carbonatites. *Fortsch. Mineral.*, **50**, 128–9.

Smith, J.V. (1995) Synchrotron X-ray sources: instrumental characteristics. New applications in microanalysis, tomography, absorption spectroscopy and diffraction. *The Analyst*, **120**, 1231–45.

Van Straaten, P. (1989) Nature and structural relationships of carbonatites from Southwest and West Tanzania. In *Carbonatites* (K. Bell, ed.)Unwin-Hyman, London, 177–99.

Veen, A.H. van der (1965) Calcite-dolomite intergrowths in high-temperature carbonate rocks. *Amer. Mineral.*, **50**, 2070–7.

Verwoerd, W.J.(1967) The carbonatites of South Africa and South West Africa. *Geol. Surv. S. Africa Handbook*, **6,** 452 pp.

Wallace, M.E. and Green, D.H. (1988) An experimental determination of primary carbonatite magma composition. *Nature*, **335**, 343–6.